energies

MDPI

Article

Investigation of Discharge Coefficients for Single Element Lean Direct Injection Modules

Han Yu, Pengfei Zhu, Jianqin Suo * and Longxi Zheng

School of Power and Energy, Northwestern Polytechnical University, Xi'an 710072, China; y_h0805@163.com (H.Y.); zpf0508@mail.nwpu.edu.cn (P.Z.); zhenglx@nwpu.edu.cn (L.Z.)
* Correspondence: jqsuo@nwpu.edu.cn; Tel.: +86-29-88431113

Received: 11 May 2018; Accepted: 12 June 2018; Published: 19 June 2018

Abstract: Lean direct injection (LDI) combustion has a high potential as a low pollution combustion method for gas turbines. The present research aims to further investigate the discharge coefficient of an LDI module, axial swirler and convergent outlet under non-reaction and reaction conditions by theoretical, numerical and experimental methods. The functional relationship between the discharge coefficient of the LDI module, axial swirler and convergent outlet was established, and the effect of swirl angle (30°, 32°, 34°, 36°, 38°, 40°) and vane number (11, 12, 13, 14, 15, 16) on discharge coefficient was studied, and finally the differences in effective flow area of LDI combustor under different inlet conditions were analyzed. The results indicate that the flow separation on the suction side increases as the swirl angle increases, which leads to a decrease of the discharge coefficient of the axial swirler, however the discharge coefficient of the convergent outlet remains unchanged first and then decreases. As the vane number increases, the flow separation on the suction side decreases and the flow friction loss increases, so that the discharge coefficient of the axial swirler and convergent outlet will first increase with the increase of vane number and then decrease with further increases. The effective flow area of combustor changes as the conditions change, but it is approximately equal under high power conditions and normal temperature and pressure conditions.

Keywords: LDI module; discharge coefficient; swirling air; convergent outlet

1. Introduction

With the increasingly stringent emission regulations on civil aircraft engines [1], modern low emission civil aircraft engines are being developed, and several low emission strategies have been successively proposed, such as Rich-burn Quick-quenching Lean-burn (RQL) [2], Lean Premixed Prevaporized (LPP) [3], and Lean Direct Injection (LDI) [4]. RQL technology may produce a large amount of NOx during the quenching process because of the occurrence of stoichiometry ratio condition. LPP technology will have low levels of emissions if the design and development are reasonable, but due to premixed and prevaporized combustion, the combustor is prone to auto ignition, flashback and combustion instability, and especially the severe combustion instability restricts the development of LPP technology. In the LDI concept, fuel and air are directly injected into the combustor, so that the auto-ignition and flashback would be avoided due to the non-premixed combustion, and the combustion instability is also not as serious as in LPP, furthermore, the LDI approach is not inferior to LPP in its ability to reduce emissions [5].

The key structure of an LDI combustor is the single element LDI module, which consists of the axial swirler, convergent outlet and nozzle. For different combustor inlet parameters, the optimized dome scheme could be obtained by varying the arrangement of LDI modules; this concept is referred to as Multi-Point Lean Direct Injection (MPLDI) [6]. For LDI combustors, the roles of the LDI module are quick mixing of fuel and air, ensuring the correct quantity of combustion air, forming the suitable

strength recirculation zone and matching with the fuel nozzle [7]. The key to ensure the quantity of combustion air is to exactly determine the discharge coefficient.

The air flow passage of the LDI module is structurally divided into a swirl flow passage and a convergent outlet. If it is considered as a whole, then it corresponds to a total discharge coefficient, which determines the flow capacity of the LDI module. The total discharge coefficient depends on the discharge coefficient of the swirler and the convergent outlet, but the relationship between them is not linear. Therefore, this paper establishes the functional discharge coefficient relationship between the LDI module, swirler and convergent outlet.

For the discharge coefficient of the swirler, Lefebvre gave the recommended values for the discharge coefficient of the axial swirler: 0.77 for flat vanes and 0.88 for curved vanes [8], however the discharge coefficient will vary with the change of geometric parameters. Shaiful [9] studied the effect of swirl number on swirler discharge coefficient with and without orifice plates. In the absence of orifice plate, the discharge coefficient decreases with the increase of swirl angle; in the case there is an orifice plate, the discharge coefficient is smaller than that without orifice plate, and decreases as the orifice decreases. Andrews [10] investigated the discharge coefficient of a radial swirler with different vane passages, including curved passage, aerodynamic tapered flat blade passage, parallel rectangular passage and circular passage. The results indicated that the swirler with parallel rectangular passage has maximum discharge coefficient, and the swirler with curved passage has minimum discharge coefficient.

For the discharge coefficient of convergent outlet, the structure of which is similar to the circular hole, many investigations were performed. Wu [11] proposed an empirical discharge coefficient model for round-hole flow, and established a functional relationship between C_d and Reynolds numbers, which can be used to predict C_d for different types of round holes. Huang [12] compared the discharge coefficient of the standard orifice and perforated orifice. The results show that the perforated orifice discharge coefficient is 22.5–25.6% higher than the standard orifice. The effect of hole thickness, number of holes, hole arrangement, and upstream disturbance on the discharge coefficient was also obtained. Singh [13] presented the experimental and numerical study on the flow meter with single-hole orifice and multi-hole orifice, it is observed that the discharge coefficient of multi-hole orifice is much larger than that of single-hole orifice. Tharakan [14] found that the back pressure has significantly effect on discharge coefficient of sharp edged injection orifices. Mazzei [15] investigated the discharge coefficient of round and inclined holes at different geometric parameters, and the correlation were proposed for predicting the discharge coefficient.

In conclusion, previous studies on swirler discharge coefficients have mainly focused on the larger size swirler, but the size of swirlers in the LDI module is much smaller than that of the conventional combustors, and the internal flow near the hub will be different from that of a large swirler. Therefore the effect of different swirl angles and the vane number on the LDI swirler discharge coefficient shall be studied in this paper. The studies on the discharge coefficient of the convergent outlet (or similar configuration) were carried out under the conditions of straight or partial upstream disturbance flow. However the upstream of the convergent outlet is in swirling flow in an LDI module, which is totally different from the straight flow. Furthermore the discharge coefficient will change with the change of swirling. Therefore, the effect of different swirl angles and vane number on the discharge coefficient of convergent outlet would be obtained in this paper. Finally, the effective flow area of combustor was investigated under different inlet conditions with and without combustion.

2. Design of LDI Module

2.1. Design Rules

The design of the LDI module is the key to the design of low emission combustors, and the following guidelines should be followed: (1) The first and most important one is to ensure the required mass flow rate, because the quantity of air that enters from the LDI module affects the amount of

combustion air, and further affects the local equivalence ratio in the combustion zone, thereby affecting the combustion reaction process and pollutant production. (2) The air flow through the LDI module should be able to form a suitable recirculation zone in the liner. The recirculation zone is the most important flow structure in the combustion chamber which plays a role in stabilizing the flame. The strength of reverse flow should neither too strong nor too weak, too strong reverse flow will cause a Processing Vortex Core (PVC), which is prone to combustion instability; too weak reverse flow cannot anchor the flame. (3) The LDI module should be able to match the nozzle. On the one hand, it means that the structure is matched, there is enough space to install and dismantle the nozzle; on the other hand, it means that fuel and air could be preferably mixed to ensure fast atomization and to form a homogeneous flammable mixture, thus avoiding the local hot points and effectively controlling the formation of pollutants.

2.2. LDI Module

The LDI module proposed in this paper consists of an axial swirler, a convergent outlet and a nozzle. As shown in Figure 1, the air enters the swirler from the inlet, and passes through the swirl vane passage to form a swirling flow, and then passes through the circular straight passage to eliminate the trailing edge of the vane, and finally forms a reasonable velocity profile at the convergent outlet. A simplex pressure atomization nozzle is installed in the center of the swirler. The nozzle outlet is flush with the convergent outlet.

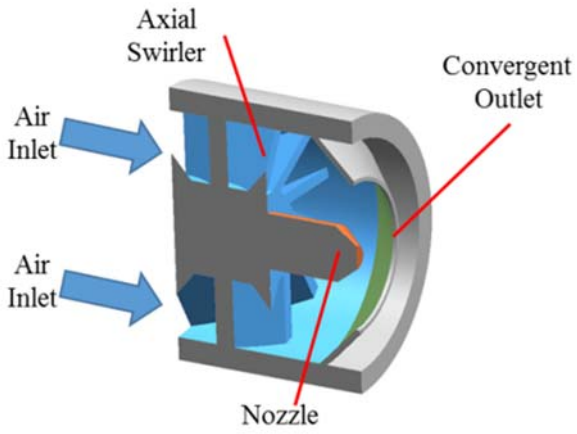

Figure 1. The LDI module.

2.3. Discharge Coefficient of LDI Module

In the design of modern combustion chambers, firstly, the total effective flow area of the combustor is calculated on the basis of the inlet and outlet parameters; and the effective flow area of each part is determined according to the air flow distribution; then the geometric area is confirmed depending on the discharge coefficient, finally the structural design is carried out by design procedures.

The LDI module is a combined flow device consisting of an axial swirler and a convergent outlet. It is the key to the design that how to determine the geometric parameters of the swirler and the convergent outlet according to the effective flow area of the entire LDI module. This requires establishing the functional relationship of the effective flow area between LDI module, axial swirler and the convergent outlet.

As shown in Figure 2, the inlet of the swirler is Section 1, the outlet of the swirler is Section 2, and the convergent outlet is Section 3.

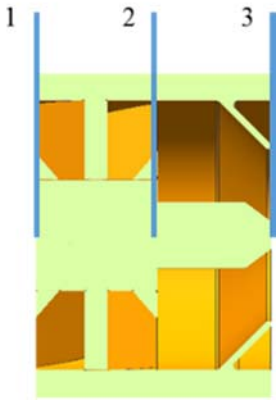

Figure 2. Three cross sections of LDI module.

The definition of the effective flow area defines by Equations (1) and (2):

$$A_{sw}C_{d-sw} = \frac{m_a}{\sqrt{2\rho(P_1^* - P_2)}} \rightarrow (P_1^* - P_2) = \frac{m_a^2}{2\rho}\frac{1}{(A_{sw}C_{d-sw})^2} \quad (1)$$

$$A_{out}C_{d-out} = \frac{m_a}{\sqrt{2\rho(P_2^* - P_3)}} \rightarrow (P_2^* - P_3) = \frac{m_a^2}{2\rho}\frac{1}{(A_{out}C_{d-out})^2} \quad (2)$$

If the LDI module is considered as a whole flow device, as Equation (3):

$$AC_d = \frac{m_a}{\sqrt{2\rho(P_1^* - P_3)}} \rightarrow (P_1^* - P_3) = \frac{m_a^2}{2\rho}\frac{1}{(AC_d)^2} \quad (3)$$

Add Equations (1) and (2) to obtain:

$$(P_1^* - P_2 + P_2^* - P_3) = \frac{m_a^2}{2\rho}\left[\frac{1}{(A_{sw}C_{d-sw})^2} + \frac{1}{(A_{out}C_{d-out})^2}\right] \quad (4)$$

It is assumed that the total pressure equals the static pressure at the exit of the swirler (Section 2), which means the dynamic pressure of this section is ignored. The rationality of this hypothesis could be explained by the results of numerical simulation, the dynamic pressure of the Section 2 only accounts for 1% of the total pressure of this section, so that the static pressure could be used instead of the total pressure. According to this hypothesis, the left side of Equation (4) can be simplified as $(P_3^* - P_1)$, and the relationship between Equations (3) and (4) can be obtained, as shown in Equation (5).

$$\frac{1}{(AC_d)^2} = \frac{1}{(A_{sw}C_{d-sw})^2} + \frac{1}{(A_{out}C_{d-out})^2} \quad (5)$$

2.4.Design Procedure

We follow these steps to design the LDI module (air alone):

- First, according to the overall design requirements of the combustion chamber and the air flow distribution of each passage, the total effective area of the LDI module is obtained, AC_d.
- Then, the relationship between the effective area of swirler ($A_{sw}C_{d-sw}$) and AC_d needs to be determined, and the ratio of $A_{sw}C_{d-sw}$ to AC_d is defined as the throttling ratio. The value of this ratio must not be less than 1.414, otherwise the flow would be throttled in the swirler. The throttling ratio is usually between 1.5 and 2.0, which means that the convergent outlet is

the throttle position of the LDI module. The larger value of the throttling ratio means that the stronger the control effect of convergent outlet on the flow capacity.

- Finally, the geometric area of the swirler and convergent outlet is determined according to C_{d-sw} and C_{d-out}.

3. Experimental Setup and Numerical Simulation Method

3.1. Geometric Model

Axial swirlers and LDI modules with different swirl angles and vane number were designed in this paper, which geometric parameters are shown in Table 1. It should be noted that the swirl angle of 34° and the vane number of 12 is a relatively common parameter settings. Therefore, the vane number is maintained at 12 when changing the swirl angle and the swirl angle is maintained at 34° when the vane number is changed.

Table 1. Parameters of axial swirlers and LDI modules.

Model \ Parameters	Axial Swirler	LDI Module
Swirl angle (°)	30~40, keep vane number is 12	
Vane number	11~16, keep swirl angle is 34°	
Hub diameter (mm)	12	
Tip diameter (mm)	33	
Vane thickness (mm)	1.25	
Vane type	Flat	
Outlet diameter (mm)	N/A	18.66
Convergent half angle (°)	N/A	45

3.2. Test Rig

The scheme of discharge coefficient test rig is shown in Figure 3.

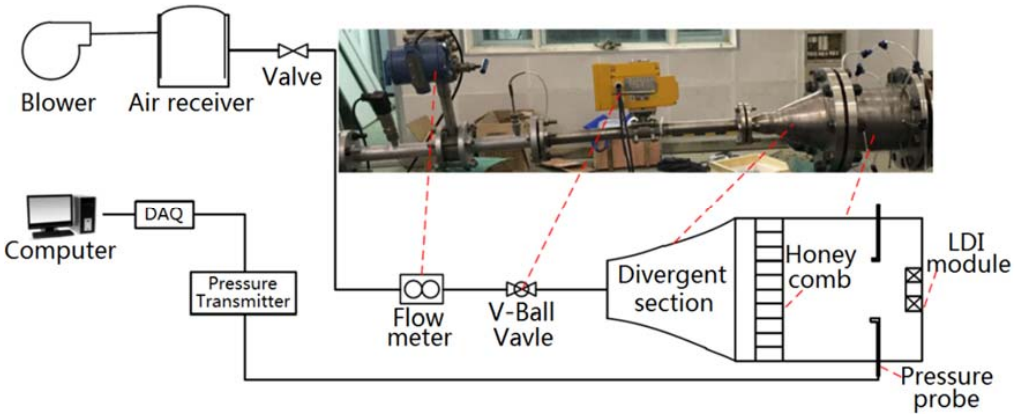

Figure 3. The schematic of test rig.

The mainstream air is provided by a twin-screw compressor, and the air flow enters the test section through the air tank and the ball valve. The air flow was measured by an orifice flow meter, whose accuracy of is 1%, and the inlet air flow was accurately adjusted through the V-ball valve. The air flow enters the measurement section through the expansion section. The honeycomb is used to straighten the air flow. Eight total pressure probes are arranged depending on equal area to obtain the average total pressure of the inlet. A Rosemount 3051S pressure transmitter measures the pressure

signal with an accuracy of 0.2%. The downstream static pressure of the LDI module is atmospheric pressure, which is measured with a MPM484 pressure transmitter with an accuracy of 0.2%.

3.3. Repeatability Analysis

A repeatability analysis was carried out for different experimental conditions to evaluate the uncertainty in the testing. The objective of this analysis is estimating the ability to maintain the experimental conditions precisely. The standard deviation of main parameters can be obtained by analysis a large number of data samples (24 samples). Results are shown in Table 2.

Table 2. Repeatability analysis.

Parameters	Units	Mean	2σ
T_{atm}	K	290.908	0.021
P_{atm}	kPa	96.006	0.066
m_a	kg/h	25.572	0.034
P_1^*	kPa	1.932	0.007
$\Delta P/P$	N/A	1.973	0.007
AC_d	mm^2	105.352	0.075

There is a 95.4% probability that the true value is less than 2σ around the mean value. The atmosphere temperature and pressure are kept constant because of the stability of transmitter. The inlet mass flow rate m_a and total pressure P_1^* show unexceptionable repeatability which can provide a stable inlet condition, furthermore, the precisely experimental conditions. The pressure drop and effective flow area also show almost no fluctuations, these indicate that the test rig could be stably operated. Therefore, the very good test data can be obtained by this experimental system.

3.4. Experimental Method

The definition of discharge coefficient is ratio of practical mass flow rate to theoretical mass flow rate, as shown in Equation (6), which is applied to any flow devices [16]:

$$C_d = \frac{m_a}{P_1^* \left(\frac{P_s}{P_1^*}\right)^{(k+1)/2k} A \sqrt{\frac{2k}{(k-1)RT_t}\left[\left(\frac{P_1^*}{P_s}\right)^{(k-1)/k} - 1\right]}} \tag{6}$$

where k is the adiabatic index, R is gas constant, m_a is the real mass flow rate, P_1^* is the average total pressure at the inlet section, P_s is the downstream static pressure, T_t is the total temperature at the inlet section, A is the geometric area of the flow passage.

The definition of discharge coefficient is ratio of practical mass flow rate to theoretical mass flow rate, as shown in Equation (6), which is applied to any flow devices. In the experimental process, the discharge coefficient of the axial swirler is first investigated to obtain the influence of the swirl angle and the vane number on the discharge coefficient. Then the effective flow area of the LDI module is obtained at different pressure drops. Finally, according to the function relationship of Equation (5), the discharge coefficient of convergent outlet would be obtained under the swirling inlet conditions with different swirl angels and vane number.

3.5. Numerical Simulation Method

The flow characteristic of single element LDI module is investigated by numerical simulation method, the purpose is to better understanding and explaining the experimental results. The ICEM CFD software is used to generate the grids of flow domain, an integrated structured grid is applied in order to improve the quality of mesh and save the storage and computation time. The Reynolds-averaged Navier-Stokes (RANS) method is applied to solve the time-averaged N-S

equations by the Fluent software; this method avoids the direct solution of N-S equations, thus greatly reducing the computational cost. And the research results show the steady-state numerical simulation could be used to predict the swirling vortex [17].

Hsiao G [18] used RANS method to simulate the swirl cup module with different turbulence models, including *standard k-epsilon*, *realizable k-epsilon*, *RNG k-epsilon*, *k-omega* and *RSM* (Reynolds Stress Equation) model. The comparison of experimental and numerical simulation results indicates that the *standard k-epsilon* model is suitable for swirler module, thus the *standard k-epsilon* model is applied in this paper. The equations are solved by SIMPLEC algorithm, the standard wall function is used and the boundary conditions are mass flow inlet and pressure outlet.

The LDI combustor model which proposed by the University of Cincinnati was used as a verification model of numerical simulation method [19]. The geometry structure of LDI module in [19] is similar to that in this paper, so that this verification has strong validity. The inlet air mass flow rate is 0.007 kg/s and the pressure drop of combustor is 4%.

The experimental (EXP) and CFD results of velocity profile are shown in Figure 4. The horizontal coordinate is a dimensionless radical position in the combustor, and the vertical coordinate is the ratio of axial velocity and reference velocity. Figure 4 shows that the CFD results are almost consistent with the EXP results. It should be noticed that there are some difference between CFD and EXP near the combustor wall; this is duo to the fact the *standard k-epsilon* model could not precisely simulate the flow near the wall. However, the air flow in near wall is not the focus in this paper, so that the numerical simulation methods could satisfy the requirement of engineering analysis.

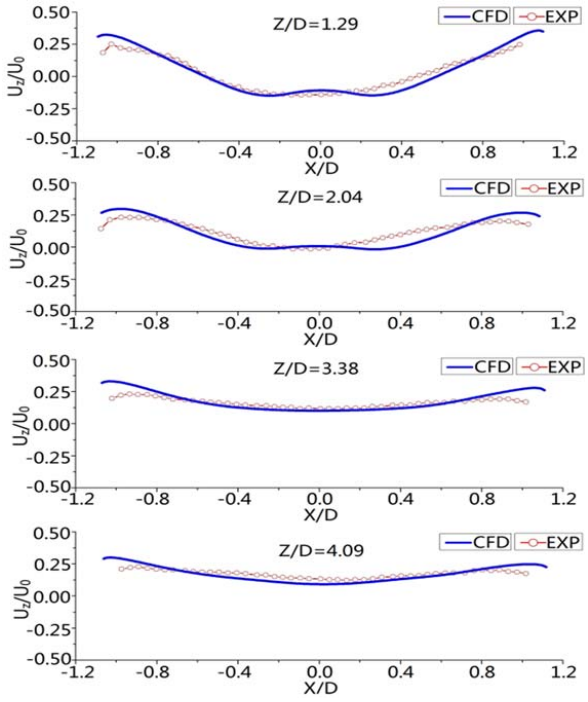

Figure 4. Compare of CFD and EXP results of velocity profile.

4. Results and Discussion

4.1. The Discharge Coefficient of Axial Swirler

4.1.1. The Effect of Swirl Angle

The effect of swirl angle on the discharge coefficient of the axial swirler is shown in Figure 5, the horizontal coordinate is the pressure drop, and the vertical coordinate is the discharge coefficient. The results show that the discharge coefficient remains almost unchanged with the increase of

pressure drop, this is because the Reynolds number is approximately 10^4 at the pressure drop is 1% in this experiment, and the discharge coefficient no longer increases when the Reynolds number is large enough.

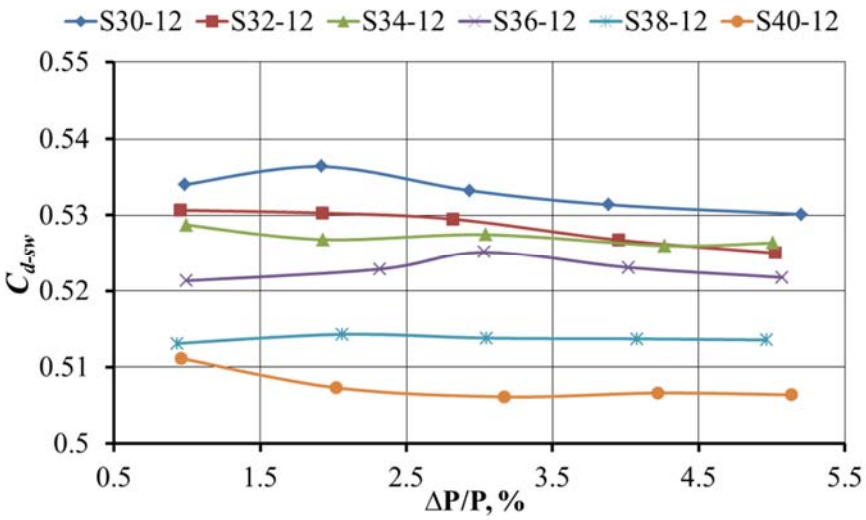

Figure 5. The effect of swirl angle on discharge coefficient of swirler.

As shown in Figure 5, the discharge coefficient of the swirler decreases as the swirl angle increases. This is because as the swirl angle increases, the airflow separation on the suction side increases, thereby the flow capability of the swirler is decreased. It should be noticed that when the pressure drop close to 5.0%, the discharge coefficient of S32-12 is slightly smaller than that of S34-12, which is different from the overall trend. This result may be due to the fact the difference of swirl angle is relatively small; furthermore, the experimental measurement accuracy is limited, thus a few abnormal data are obtained. However, the overall trend could be still hold.

In order to further understand the experimental results, the numerical simulations of LDI modules with typical swirling angles were performed, the result is shown in Figure 6.

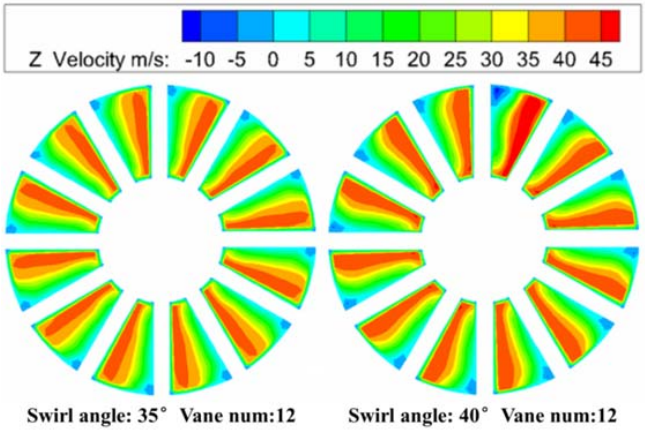

Figure 6. Comparison of airflow separation degree on suction side with different swirl angles.

This is the axial velocity contour in the vane passage of the swirler when the swirl angle is 35° or 40°. The results indicated that the velocity difference between the suction side and pressure side is larger when the swirl angle is 40°, which indicated that the 40° swirler has a greater airflow separation.

From the experimental results in [9], it can also be seen that the discharge coefficient decreases significantly with the increase of swirl angle. However, the discharge coefficients obtained for the swirler with the same swirl angle in this paper are smaller than those in the literature, because the size of the swirlers in this paper are much smaller than that of the swirler in [9]. In the case of a small scale swirler, the vanes are denser at the hub, so that the flow capacity is weaker than that of a large scale swirler.

4.1.2. The Effect of Vane Number

The effect of vane number on swirler discharge coefficient is shown in Figure 7. The horizontal coordinate is the pressure drop, and the vertical coordinate is the discharge coefficient. The discharge coefficient is almost unchanged with the increase of pressure drop, for the same reason as in Figure 5. As the vane number increases, the discharge coefficient first increases and then decreases, reaching the maximum at 15 vanes. It should be noticed that when the pressure drop is large than 4.0%, the discharge coefficient of S34-13 and S34-14 are approximately equal, which is different from the overall trend. The reason of this result is similar to the Section 4.1.1; however, the overall trend could also still be obtained.

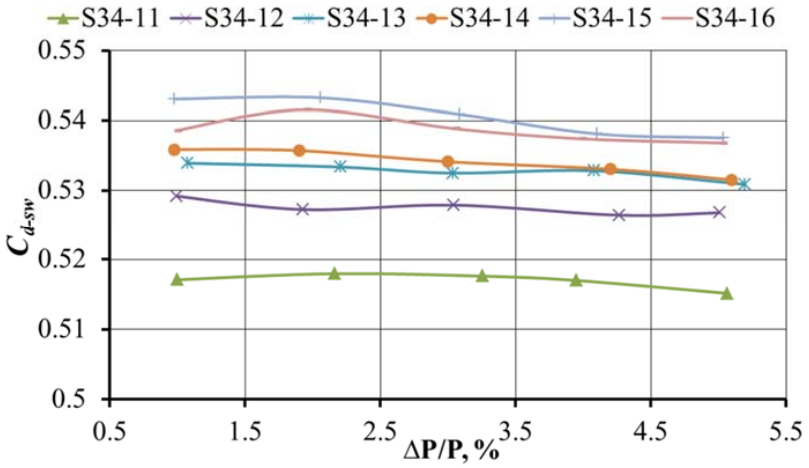

Figure 7. The effect of vane number on discharge coefficient.

The influence of the vane number on the discharge coefficient of the swirler is mainly reflected in two aspects: (1) For a certain swirl angle, as the vane number increases, the airflow separation on the suction side of the vane gradually decreases, resulting in an increased flow capacity of the swirler, so that the discharge coefficient increases. (2) As the vane number increases, the surface area of the flow passage also increases, resulting in an increase in the friction loss between the fluid and the wall, which reducing the flow capacity of the swirler, therefore decreasing the discharge coefficient. Considering the above two factors in a comprehensive manner, when the vane number is small, the airflow separation plays a leading role in the flow capacity. When the vane number is large, the degree of airflow separation will not be significantly improved, but the influence of friction loss on discharge coefficient plays a leading role.

4.2. The Discharge Coefficient of Convergent Outlet under Swirling Inlet Conditions

The flow characteristic of the LDI module was tested at the same inlet conditions. The effect of swirl angle and vane number on effective flow area was obtained under different pressure drops, according to the discharge coefficient results of axial swirler, the effective flow area of convergent outlet is calculated by solving the Equation (5), and then the discharge coefficient of convergent outlet is obtained according to the geometry area.

4.2.1. The Effect of Swirl Angle

The relationship between the discharge coefficient of convergent outlet and the swirl angle at different air flow rates (corresponding to different pressure drops) is shown in Figure 8. As the swirl angle increases, the C_{d-out} almost unchanged until the swirl angle is greater than 36°, C_{d-out} decreases significantly and reaches a minimum value at a swirl angle of 40°.

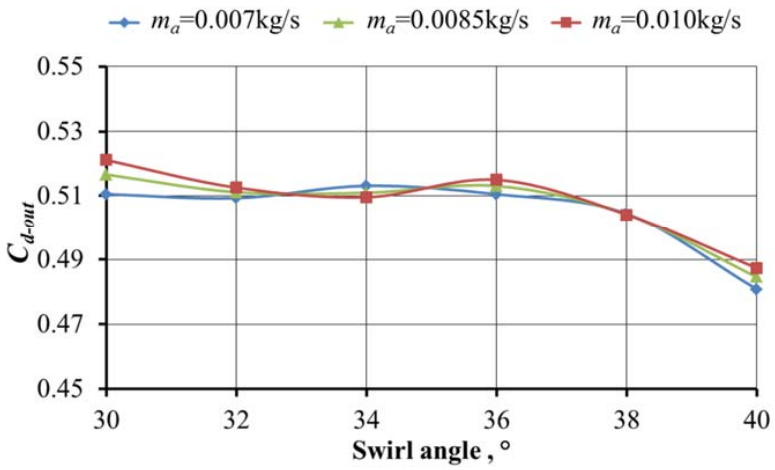

Figure 8. The effect of swirl angle on discharge coefficient of convergent outlet.

Figure 8 needs to be explained: (1) The convergent outlet could be considered as a circular hole, according to previous studies [13], if the air flow is straight at the inlet, the discharge coefficient of single-hole orifice is around 0.67. However, the discharge coefficient is significantly decreased under the swirl flow inlet conditions. This is because the swirl flow has a large tangential velocity compared to the straight flow, and the air flows radially outwards under the action of the centrifugal force, resulting in the decrease of the flow capacity, so the discharge coefficient is reduced. (2) When the swirl angle is greater than 36°, the discharge coefficient begins to drop significantly. This is because as the swirling flow gradually increases, vortex breakdown occurs at downstream of the convergent outlet, as shown in Figure 9b, the vortex breakdown appears as a stagnation point in the flow field, the stagnation point is followed by the center recirculation zone. The vortex breakdown bubble (VBB) in the flow field is equivalent to an obstacle [17], so the air will flow to the outside under the effect of VBB, further reducing its central flow capacity. When the swirling intensity is weak, as shown in Figure 9a, the swirling flow is not sufficient to form a central recirculation zone that blocks the flow in the downstream, so the discharge coefficient of the convergent outlet under the weak swirling flow is larger than that under the strong swirling flow.

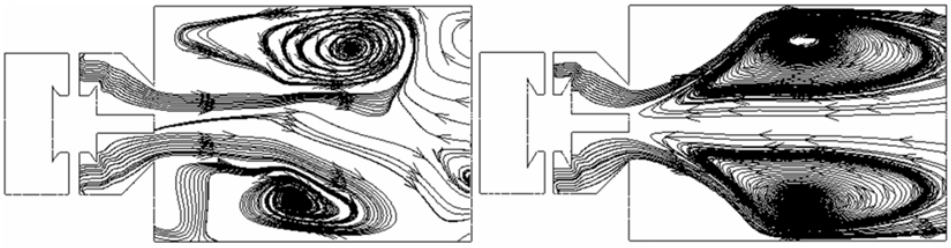

Figure 9. The streamline of combustor at different swirling intensity.

4.2.2. The Effect of Vane Number

The relationship between the discharge coefficient of convergent outlet and the vane number at different air flow rates (corresponding to different pressure drops) is shown in Figure 10. With the increase of the vane number, C_{d-out} tends to increase first and then decreases.

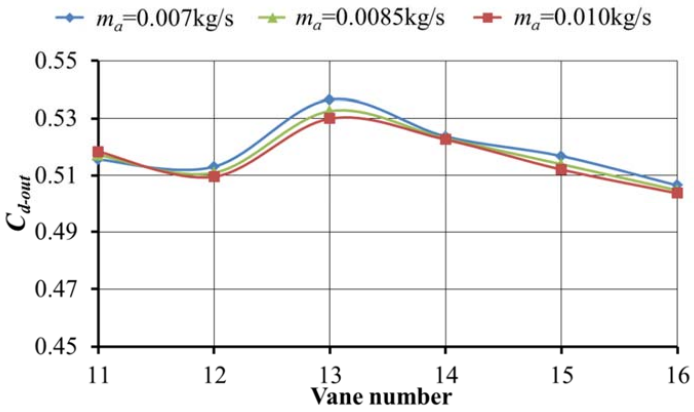

Figure 10. The effect of vane number on discharge coefficient of convergent outlet.

This is because with the increase of the vane number, the degree of separation of the airflow on the suction side of the vanes gradually decreases, resulting in the increase of swirling intensity, and the radial distribution of axial velocity in the section of convergent outlet is changed. When the swirling intensity is weak, the airflow is concentrated at the position near the center, the velocity distribution curve is of the type of "inner high, outer low", and with the increase of the swirling intensity, and the airflow begins to move radially outwards. Meanwhile the speed near the inside gradually decreases, and the speed near the outside gradually increases, resulting in the discharge coefficient increases. When the swirling intensity is strong enough to form the recirculation zone in the downstream, the discharge coefficient begins to decrease.

4.3. The Effective Flow Area of LDI Module under Non-Reaction and Reaction Conditions

The gas turbine combustor is operating at high inlet temperature and pressure conditions, but the above investigations of discharge coefficient were carried out under normal temperature and pressure, which raises a question: whether the experimental results obtained at normal temperature and pressure conditions are still applicable at high temperature and pressure conditions with combustion. Therefore, in order to investigate the effective flow area of combustor under combustion conditions, the single-tube LDI combustor was proposed, as shown in Figure 11, the combustor consists of LDI module, liner, casing and dome flange.

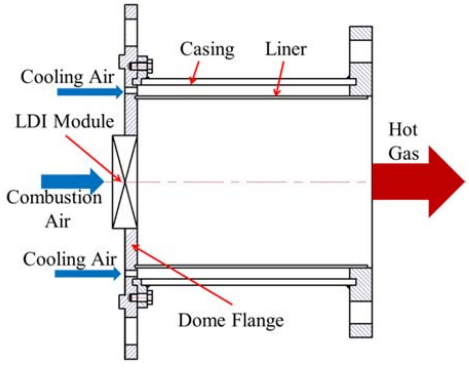

Figure 11. The LDI single tube combustor.

The experiments were performed under three conditions:

1. Normal temperature and pressure without combustion (AC_{d1});
2. Normal temperature and elevated pressure without combustion (AC_{d2});
3. Elevated temperature and pressure with combustion (AC_{d3}).

The results are shown in Figure 12, the horizontal ordinate is the ratio of Fuel Air Ratio (FAR) to Burner Inlet Temperature (BIT), which indicates the ratio of temperature rise to BIT ($(T_{t4} - T_{t3})/T_{t3}$). The FAR/BIT affects the combustor pressure loss due to combustion, and then affects the effective flow area. The vertical ordinate is effective flow area.

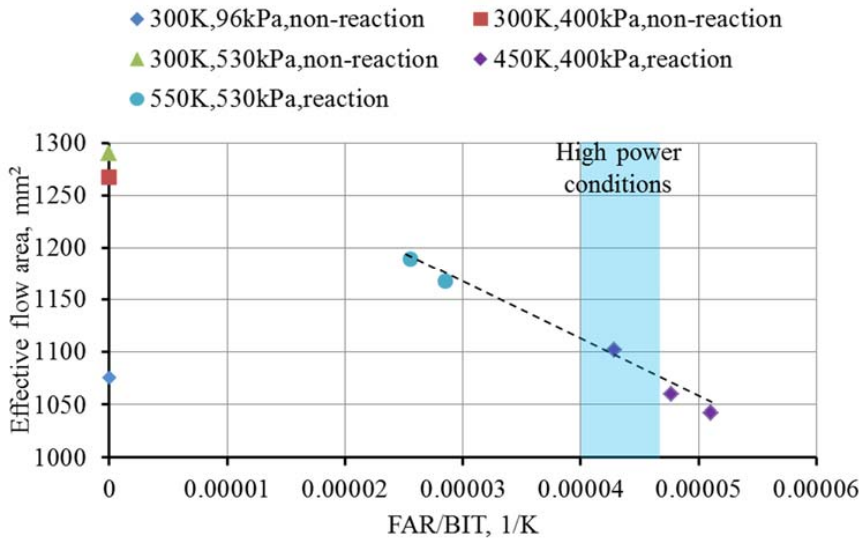

Figure 12. Compare of effective flow areas under different conditions.

The following conclusion can be drawn from Figure 11:

1. AC_{d2} is significantly larger than AC_{d1}, this is because the Reynold number of the combustor increases as the inlet pressure increases, and then the effective flow area increases. However, the effective flow area no longer increases when the Reynold number is large enough.
2. AC_{d3} is smaller than AC_{d2}, this is due to the thermal resistance caused by the combustion reaction, resulting in the increase of combustor pressure loss. And as the FAR/BIT increases, the heat release also increases, resulting in the decrease of effective flow area.
3. The FAR/BIT range corresponding to the high power conditions of LDI combustor in this paper is approximately the blue area in the Figure 11 (Inlet temperature: 750 K, total FAR: 0.030–0.035). The effective flow areas of combustor are approximately equal at high power conditions and normal temperature and pressure conditions, that means the experimental results that obtained at normal temperature and pressure conditions are still applicable at high temperature and pressure conditions with combustion.

5. Conclusions

Following conclusions are obtained in this paper:

1. The functional relationship of effective area between LDI module, swirler, and convergent outlet is established based on the reasonable hypothesis, and the primary design procedure of LDI module is given.
2. The discharge coefficient of small scale axial swirler is less than that of large scale swirler. As the swirl angle increases, the discharge coefficient decreases due to the increase of the

airflow separation on the suction side; as the vane number increases, the airflow separation decreases, but the airflow friction increases, resulting in the fact that the discharge coefficient shows an increase trend first and then decreases.

3. The discharge coefficient of a convergent outlet under swirling air inlet is obviously smaller than that of the straight flow inlet, which is mainly affected by the velocity profile of the upstream and downstream flow field. As the swirl angle and vane number change, the discharge coefficient decreases when the recirculation zone is formed downstream of the module.
4. The effective flow areas of the combustor are approximately equal under high power conditions and normal temperature and pressure conditions. This indicates that the investigation of discharge coefficient could be carried out under normal temperature and pressure conditions.

Author Contributions: Investigation, Writing-Original Draft Preparation, H.Y.; Data Curation, P.Z.; Resources, J.S.; Supervision, L.Z.

Acknowledgments: We are very grateful to J. S. Chin (AIAA Associate Fellow) for his help of technical guidance and English writing.

Conflicts of Interest: The authors declare no conflict of interest.

Nomenclature

A	Geometric area
A_{out}	Convergent outlet area
A_{sw}	Swirler area
AC_{d1}	Effective flow area of combustor (normal temperature and pressure without combustion)
AC_{d2}	Effective flow area of combustor (normal temperature and elevated pressure without combustion)
AC_{d3}	Effective flow area of combustor (elevated temperature and pressure with combustion)
BIT	Burner inlet temperature
C_d	Discharge coefficient
C_{d-out}	Discharge coefficient of convergent outlet
C_{d-sw}	Discharge coefficient of swirler
FAR	Fuel air ratio
k	Adiabatic index
m_a	Air mass flow rate
P_1^*	Total pressure on Section 1
P_2	Static pressure on Section 2
P_2^*	Total pressure on Section 2
P_3	Static pressure on Section 3
P_{atm}	Atmosphere pressure
P_s	Downstream static pressure
R	Gas constant
T_{atm}	Atmosphere temperature
T_t	Inlet temperature
$\Delta P/P$	Pressure drop

References

1. Lieuwen, T.C.; Yang, V. *Gas Turbine Emissions*; Cambridge University Press: Cambridge, UK, 2013; pp. 86–93. ISBN 978-0-521-76405-6.
2. Mckinney, R.; Cheung, A.; Sowa, W. The Pratt & Whitney TALON X Low Emissions Combustor: Revolutionary Results with Evolutionary Technology. In Proceedings of the 45th AIAA Aerospace Sciences Meeting and Exhibit, Reno, NV, USA, 8–11 January 2007.
3. Foust, M.; Thomsen, D.; Stickles, R.; Cooper, C.; Dodds, W. Development of the GE Aviation Low Emissions TAPS Combustor for Next Generation Aircraft Engines. In Proceedings of the AIAA Aerospace Sciences Meeting, Grapevine, TX, USA, 7–10 January 2013.

4. Lee, C.M. NASA Project Develops Next Generation Low-emissions Combustor Technologies. In Proceedings of the AIAA Aerospace Sciences Meeting, Grapevine, TX, USA, 7–10 January 2013.
5. Dewanji, D. Flow Characteristics in Lean Direct Injection Combustors. *J. Propul. Power* **2012**, *28*, 181–196. [CrossRef]
6. Tacina, R.; Wey, C.; Laing, P.; Mansour, A. Sector Tests of a Low NOx, Lean-Direct-Injection, Multipoint Integrated Module Combustor Concept. In Proceedings of the ASME Turbo Expo, Amsterdam, The Netherlands, 3–6 June 2002.
7. Khandelwal, B.; Dong, L.; Sethi, V. Design and Study on Performance of Axial Swirler for Annular Combustor by Changing Different Design Parameters. *J. Energy Inst.* **2014**, *87*, 372–382. [CrossRef]
8. Lefebvre, A.H.; Ballal, D.R. *Gas Turbine Combustion*; CRC Press: Boca Raton, FL, USA, 2010.
9. Shaiful, M.; Mohd, M.N. The Effect of Swirl Number on Discharge Coefficient for Various Orifice Sizes in a Burner System. *Jurnal Mekanikal* **2004**, *17*, 99–108.
10. Andrews, G.E.; Escott, N.; Mkpadi, M.C. Radial Swirler Designs for Ultra-Low NOx Gas Turbine Combustion. In *ASME Turbo Expo: Power for Land, Sea, and Air*; American Society of Mechanical Engineers: New York, NY, USA, 2008; pp. 277–289.
11. Wu, D.; Burton, R.; Schoenau, G. An Empirical Discharge Coefficient Model for Orifice Flow. *Int. J. Fluid Power* **2002**, *3*, 13–19. [CrossRef]
12. Huang, S.; Ma, T.; Wang, D.; Lin, Z. Study on Discharge Coefficient of Perforated Orifices as a New Kind of Flowmeter. *Exp. Therm. Fluid Sci.* **2013**, *46*, 74–83. [CrossRef]
13. Singh, V.K.; Tharakan, T.J. Numerical Simulations for Multi-hole Orifice Flow Meter. *Flow Meas. Instrum.* **2015**, *45*, 375–383. [CrossRef]
14. Tharakan, T.J.; Rafeeque, T.A. The Role of Backpressure on Discharge Coefficient of Sharp Edged Injection Orifices. *Aerosp. Sci. Technol.* **2016**, *49*, 269–275. [CrossRef]
15. Mazzei, L.; Winchler, L.; Andreini, A. Development of a Numerical Correlation for the Discharge Coefficient of Round Inclined Holes with Low Crossflow. *Comput. Fluids* **2017**, *152*, 182–192. [CrossRef]
16. Gritsch, M.; Saumwebber, C. Effect of Internal Coolant Cross-flow Orientation on the Discharge Coefficient of Shaped Film-cooling Holes. *ASME J. Turbomach.* **2000**, *122*, 146–152. [CrossRef]
17. Lieuwen, T.C. *Unsteady Combustor Physics*; Cambridge University Press: Cambridge, MA, USA, 2012; ISBN 978-1-107-01599-9.
18. Hsiao, G.; Mongia, H. Swirl Cup Modeling Part 3: Grid Independent Solution with Different Turbulence Models. In Proceedings of the 41st Aerospace Sciences Meeting and Exhibit, Reno, NV, USA, 6–9 January 2003.
19. Fu, Y. Aerodynamics and Combustion of Axial Swirlers. Ph.D. Thesis, Cincinnati University, Cincinnati, OH, USA, 2008.